Chapter 9

# Post-Incipience Cavitation Evolution of an Eccentric Journal Bearing

Coda H.T. Pan and Daejong Kim

Additional information is available at the end of the chapter

http://dx.doi.org/10.5772/intechopen.80842

**Abstract**

Hypothesis of Gümbel is a statement of the initial state of an incompressible fluid film as governed by the hyperbolic differential equation. Olsson's interphase condition, upon providing cross-boundary interface continuity, targets the Swift-Stieber state at the rupture boundary with a nonvanishing speed that is a function of the postulated cavitation morphology model; experimental photographic records suggest the rolling stream concept which combines an adhered film immediately downstream of the boundary and striated streams farther on. To study cavitation without end-leakage effects, the pre-incipience contiguous fluid film solution is given by the Sommerfeld solution with the ambient state and is reduced to the π-film, and the issue of post-incipience evolution is reduced to an appropriate interpretation of a suitably defined evolution time. To treat cavitation with allowance for end-leakage effects, computation of the pre-incipience contiguous film requires a two-dimensional adaptation of the Sommerfeld solution with a consistent spline interpolation scheme, and treatment of Olsson's interphase condition is quite elaborate.

**Keywords:** journal bearing, cavitation, hyperbolic differential equations, morphology

## 1. Introduction

### 1.1. JFO dissertation reports

Popularly recognized acronym **JFO** is used to represent three important dissertation reports published by Chalmers University of Technology that summarize the monumental effort of Prof. Bengt Jakobsson:

- Floberg [1] examined the Sommerfeld-Gümbel issue, noting symmetry properties that can be associated with the film thickness function and the possibility of suppressing cavitation via an elevated bias pressure in the absence of end leakage.
- Jakobsson and Floberg [2] resorted to adoption of a relaxation procedure of the 5-point type, using midpoint Poiseuille flux in the circumferential direction and claimed to be more accurate than the Christopherson algorithm [3] to deal with side leakage for bearings of finite length; occurrence of cavitation was modeled as the suppression of the Poiseuille flux component. Various ways of fluid supply were considered.
- Olsson [4] turned attention to dynamically loaded bearings; allowing for time-dependence, the void boundary was required to move to maintain fluid continuity. The concept of "fractional width of oil strip" was introduced to characterize the cavitated fluid. Olsson mentioned the possibility of an adhered moving film but tacitly chose not to treat it. The condition of Swift [5] and Stieber [6] is regarded to be prerequisite.

### 1.2. Morphology of cavitated fluid

Photographs of striated cavitated pattern are commonly cited as validation of the morphology model of narrow oil strips shown in **Figure 1(a)**; Pan et al. [9] suggested an alternative interpretation as depicted in **Figure 1(b)**, and the two-component rupture front describes shear sheets interspersed by wet voids that emerge in the form of a moving adhered film. The oil strip morphology model presents an awkward prerequisite of the Swift-Stieber condition that is not achievable.

### 1.3. Olsson's interphase condition

Olsson derived an interphase condition (**OIC**) across a void boundary that requires the void boundary to move to maintain fluid-gas continuity. The symbol $\Theta$ was introduced to represent fractional content of fluid in the film space in the cavitated region. He noted that the motion of either boundary can be treated by the method of characteristics for hyperbolic differential equations.

The one-dimensional form of **OIC** is

$$(1 - \Theta_\Sigma)\dot{\theta}_\Sigma = (\Phi_{\theta;\Sigma}/H_\Sigma) - \Theta_\Sigma \tag{1}$$

Regardless of the morphology model, an exact analytical integral of the above equation is contradictory to the Swift-Stieber condition!

**OIC** was used indiscriminately to model dynamic performance of heavily loaded reciprocating engine bearings. Realization of the past wasted effort is ample motivating impetus for the present work.

### 1.4. Rolling stream cavitation morphology

Primarily concerned with the 1-D Swift-Stieber evolution process, Pan et al. [9] advocated the rolling stream cavitation morphology that makes use of a two-component rupture front

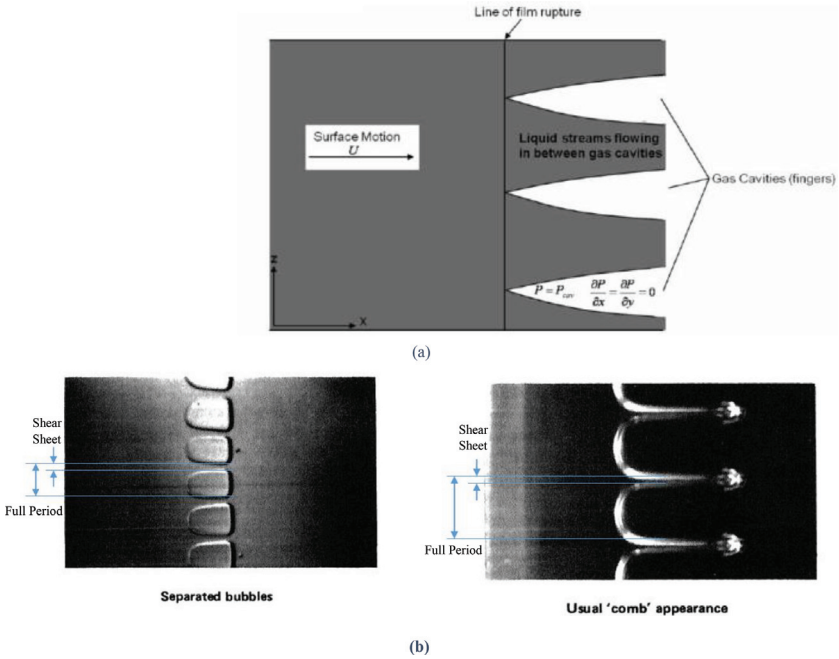


**Figure 1.** Alternative interpretations of striated void patterns. (a) Narrow oil strip model of Jakobsson and Floberg [2] as sketched in Braun and Hannon [7]. (b) Photographs after Dowson and Taylor [8] depicted as the model of two-component rupture front.

description of the cavitated fluid film; $1.0 > \Theta_\Sigma > 0.0$ is the width fraction of the wet shear sheet illustrated in **Figure 1(b)**. The latter value requires a satisfactory resolution of the problem posed by Savage [10].

### 1.5. Cross-boundary interface condition

Pan et al. [9] reasoned that the flow crossing the moving rupture boundary is same as that of the cavitated fluid that enters the ruptured region; therefore, in place of Eq. (1), cross-boundary interface condition (**CBIC**) is proposed:

$$\begin{aligned}(1-\Theta_\Sigma)\dot{\theta}_{\Sigma\mathrm{CBIC}} &= 1 - H_\Sigma^2(\partial P/\partial\theta)_\Sigma \\ \dot{\zeta}_{\Sigma\mathrm{CBIC}} &= -H_\Sigma^2(\partial P/\partial\zeta)_\Sigma\end{aligned} \tag{2}$$

**CBIC** targets the Swift-Stieber condition at the rupture boundary.

## 2. Post-incipience cavitation evolution

The classical Sommerfeld solution [11] was cited by Gümbel [12], noting that sub-ambient film pressure had not been observed in experiments. The path of an evolution process is due to the

celebrated Swift-Stieber condition [5, 6]. Gümbel's hypothesis to ignore sub-ambient part of the 1D Sommerfeld solution can be generalized to apply to a properly computed contiguous journal bearing film. Equation (2) is the characteristic formula of the post-incipience evolution. Following Gümbel's hypothesis with a complete initial value specification deals with the hyperbolic differential equation noted by Olsson.

### 2.1. Rolling stream cavitation morphology (initial $\Theta_{\Sigma\ \mathrm{CBIC}}$)

The rolling stream cavitation morphology uses a two-component rupture front description of the cavitated fluid film; $1.0 > \Theta_\Sigma > 0.0$ would be used to illustrate the influence of the unknown parameter.

While **CBIC** governs the rupture boundary, the formation boundary motion derived in **OIC** remains valid:

$$\begin{aligned}(1-\Theta_{\text{formation}})\dot{\theta}_{\text{formation}} &= \Phi_{\theta;\,\text{formation}}/H_{\text{formation}}\\ (1-\Theta_{\text{formation}})\dot{\zeta}_{\text{formation}} &= -H_{\text{formation}}^{-2}\left(\partial P/\partial\zeta|_{\text{formation}}\right)\end{aligned} \tag{3}$$

For the 1D problem, pursuant to Gümbel's hypothesis, $\tau$- stepping both boundaries in synchronism from $\tau = 0.0$ with an assigned $\delta\tau$:

$$\begin{aligned}\theta_{\Sigma\,\text{CBIC}} &= \left(1-\overline{\Theta}_\Sigma\right)^{-1}\left\{1-\frac{1}{2}\left[\sum_{\kappa=0}^{1}H_\Sigma^2(\partial P/\partial\theta)_\Sigma\right]_{\kappa\delta\tau}\right\}\\ \theta_{\text{formation}} &= \left(1-\overline{\Theta}_{\text{formation}}\right)^{-1}\frac{1}{2}\left[\sum_{\kappa=0}^{1}H_{\text{formation}}^2(\partial P/\partial\theta)_{\text{formation}}\right]_{\kappa\delta\tau}\end{aligned} \tag{4}$$

$\overline{\Theta}_\Sigma$, $\overline{\Theta}_{\text{formation}}$ and $\frac{1}{2}\left[\sum_{\kappa=0}^{1}H^2(\partial P/\partial\theta)\right]_{\kappa\delta\tau}$ are algebraic mean approximations; Swift-Stieber condition targets the Sommerfeld invariant $\Phi_{\theta;\,\text{rupture}} = H_{\text{rupture}} = \left(1-\varepsilon^2\right)/\left(1+\varepsilon^2\right)$ with accuracy no better than the floating-point word processor precision, typically $o\{10^{-14}\}$. The evolution trajectory is dependent on the initial $\Theta_\Sigma$.

If the initial $\Theta_\Sigma <\!\!\rightarrow 1.0$ Swift-Stieber condition is satisfied at nil $\tau$, trajectory time scale is expanded by a factor of $1-\Theta_{\text{rupture CBIC}}$, and the formation boundary is regarded to be immobile in the expanded time scale. For all other initials $1.0 > \Theta_\Sigma > 0.0$, the same Sommerfeld invariant is targeted, the formation boundary would move into the divergent semicircle, and the evolution trajectory is regarded to have reached the asymptotic Swift-Stieber condition when the most recent $\tau$- step yielded less than $o\{10^{-14}\}$ formation boundary shift.

### 2.2. Computation of the contiguous film (LGCMIED)

The presence of end-leakage flow calls for $\dot{\zeta}_{\text{rupture CBIC}}$ and $\dot{\zeta}_{\text{formation}}$, respectively, by **CBIC** and **OIC**. A new computation algorithm was introduced [13] to execute Eqs. (2) and (3). **LGCMIED**, used as acronym for Liquid-film Grid-Centered Mesh Integral Emulation of flux Divergence,

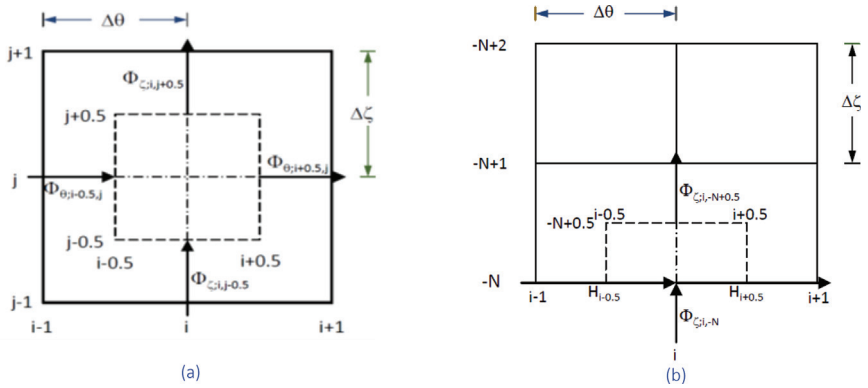


**Figure 2.** **LGCMIED** scheme: (a) internal grid and (b) boundary grid.

divergence emulation can be constructed around the dash-line peripheries of the central cell illustrated in from mid-mesh fluxes $\Phi_{\theta;\, i\mp 0.5,\, j}$ and $\Phi_{\zeta;\, i,\, j\mp 0.5}$. Extending to 2D problems, side-leakage fluxes would be computed according to the illustration of **Figure 2(b)**.

### 2.3. Lubricant circulation

In **Figure 2(b)**, as illustrated, $\Phi_{\zeta;\, i,\, -N}$ is directed into the fluid film representing a feeding function; if a reverse direction is indicated, then the cross-end-boundary process represents a draining function. Two combinations are possible, either feed-feed or feed-drain.

The feed-feed arrangement with both ends maintained at atmospheric ambient is the π-film. Perfect ζ-symmetry is seen in all flux profiles; slight 2D attribute is seen in slight convexity in $\Phi_{\theta;\, \text{rupture}}$ and concavity in $\Phi_{\theta;\, \text{formation}}$ (see **Figure 3**).

### 2.4. Feed pressurization

In the feed-drain arrangement, feed lubricant pressurization is a design feature of considerable importance. Increased through-flow by pressurization is potentially a way to meet a heavy duty application. For a very small $P_{\text{feed}}$, e.g., $10^{-6}$, void boundaries and peripheral fluxes are graphically not distinguishable from those of the π-film.

For a moderately larger $P_{\text{feed}}$, e.g., $10^{-3}$, void boundaries and peripheral fluxes, as shown in **Figure 5**, are quite different.

Void feeding flow is computed by adapting the short-bearing approximation of Michell [14].

Bearing in mind that $P_{\text{peak}}$ of the Sommerfeld solution is 2.160137, feed pressure effects for $P_{\text{feed}} = 10^{-3}$ are remarkably prominent. Etsion and Ludwig [15] reported on measurement of fluid film inertia effects in the submerged operation of a cavitated journal bearing in a self-induced oscillating mode. The pronounced feed pressurization features shown in **Figure 5** may

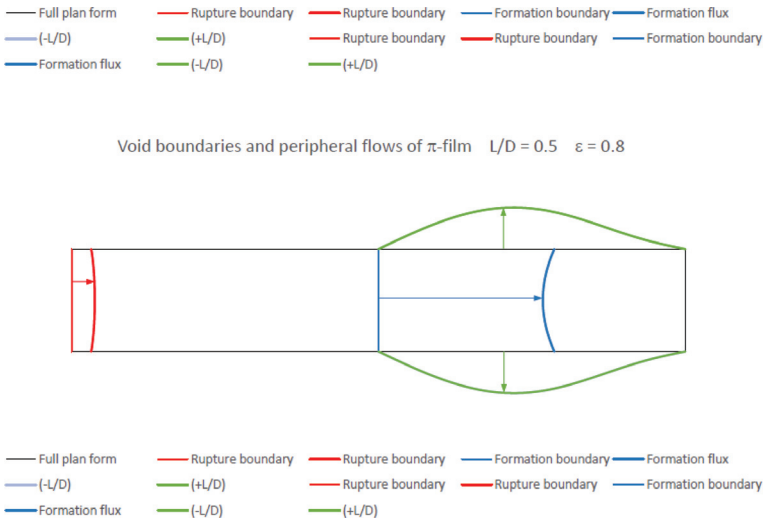


**Figure 3.** Void boundaries and peripheral fluxes of π-film.

prevent establishment of the asymptotic Swift-Stieber condition but develop a self-induced limit cycle oscillation; **CBIC** always targets the Swift-Stieber condition, but the asymptotic state is not guaranteed.

**Figures 3–6** are computed immediately upon accepting Gümbel's hypothesis to initiate post-incipience cavitation evolution. Treatment of the 2-D aspect of Eq. (2) regarding $\dot{\zeta}_{\Sigma CBIC}$, a high order $\tau$-stepping iterative procedure is required [16].

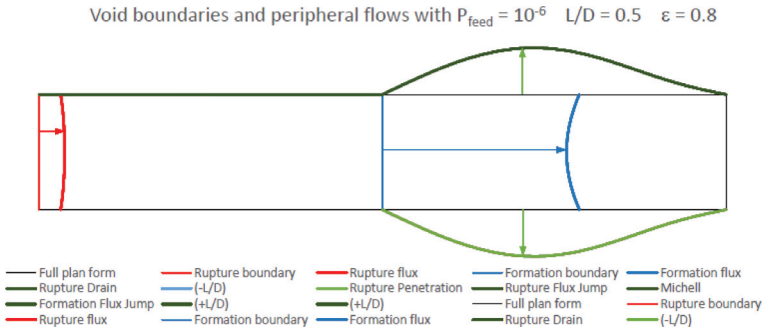


**Figure 4.** Void boundaries and peripheral fluxes with $P_{feed} = 10^{-6}$.

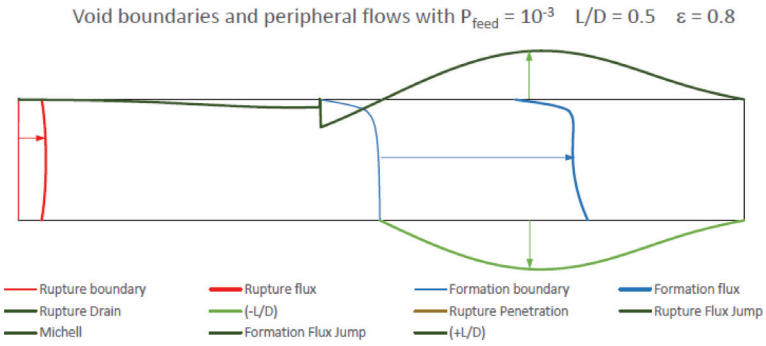


**Figure 5.** Void boundaries and peripheral fluxes with $P_{feed} = 10^{-3}$.

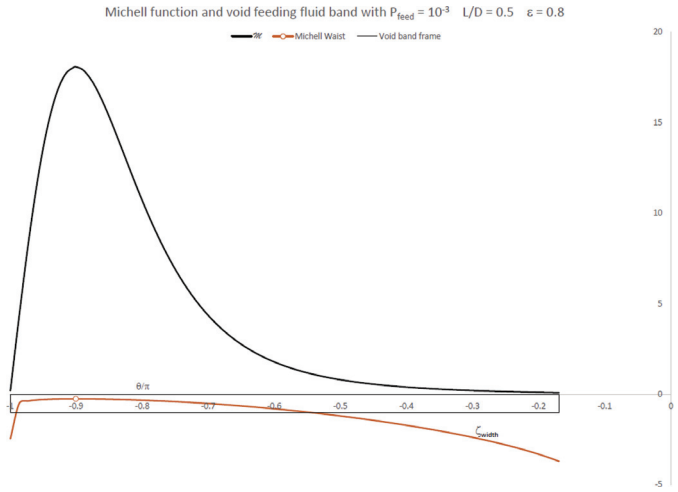


**Figure 6.** Michell function (void feeding).

## 2.5. Spline-smoothed LGCMIED

Consolidating divergence emulation at both central and boundary grids, contiguously blended $\Phi_{\zeta;i,j}$, can be compiled as shown in **Figure 7**. Each "curve" is nearly a straight line. A third-order polynomial curve fit connects upper and lower parts of the bearing. Line plotting is used to bring out "kinks" in first-order spline blending in connecting mid-mesh and grid point values. To carry out smooth Swift-Stieber targeting with $\Theta_{\Sigma} < 1.0$, second-order spline blending is necessary [17].

Spline interpolation of $\Phi_{\theta}$ is performed at $\zeta_{\text{CBIC interpolated}}$.

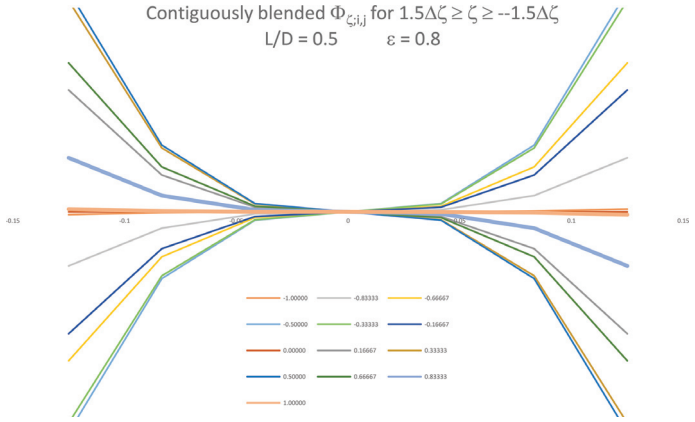


**Figure 7.** Axial-blended $\Phi_{\zeta;i,j}$.

## 3. Summary

1. **CBIC** is used to target the Swift-Stieber condition at the rupture boundary.
2. Gümbel's hypothesis is extended to allow 2D treatment in conjunction with computation of contiguous films with LGCMIED algorithm.
3. The two-component rupture front description of the cavitated fluid film; $1.0 > \Theta_{\Sigma} > 0.0$ is an unknown parameter. $\Theta_{\Sigma} < \rightarrow 1.0$ would yield the asymptotic Swift-Stieber state.
4. In 1D problems, a universal post-incipience cavitation evolution is $\tau$-stepped according to an assumed $\Theta_{\Sigma}$.
5. In 2D problems, it is necessary to specify lubricant circulation roles of the two bearing ends:
   - Feed-feed
   - Feed-drain
6. Feed pressurization is represented by an elevated $P_{\text{feed}}$.
7. Sample contiguous film calculation immediately following Gümbel's hypothesis represents the beginning of post-incipience cavitation evolution.

## Nomenclature

### Roman letters

| | |
|---|---|
| $C$ | radial bearing clearance, m |
| $e$ | journal eccentricity, m |

| | |
|---|---|
| $H$ | nondimensional film thickness, = 1 + $\varepsilon$ cos$\theta$ |
| $i, j,k$ | Cartesian unit base vectors |
| $M$ | number of circumferential mesh spacings in a semicircular span |
| $N$ | number of axial mesh spacings across one-half length of the bearing |
| $P$ | nondimensional film pressure, $= 6\mu\omega(R/C)^2 p$ |
| $p$ | film pressure above ambient, pascal |
| $t$ | time, s |
| $x, y, z$ | Cartesian coordinates, m |

**Greek letters**

| | |
|---|---|
| $\varepsilon$ | bearing eccentricity ratio, = $e/C$ |
| $\vec{\Phi}$ | nondimensional flux vector, $= \vec{i}\ \Phi_\theta + \vec{k}\ \Phi_\zeta$ |
| $\Phi_{\Sigma;\theta}$ | nondimensional cross-void circumferential flux |
| $\Theta_\Sigma$ | fluid fraction of cavitated film at void boundary |
| $\theta$ | circumferential coordinate, radian |
| $\theta_\Sigma$ | circumferential location of void boundary, radian |
| $\dot{\theta}_\Sigma$ | non dimensional circumferential speed of void boundary |
| $\Delta\theta$ | circumferential mesh spacing |
| $\tau$ | nondimensional time, $= \frac{1}{2}\omega t$ |
| $\omega$ | journal rotational rate, rad/s |
| $\zeta$ | nondimensional axial coordinate |
| $\zeta_\Sigma$ | axial location of void boundary |
| $\dot{\zeta}_\Sigma$ | nondimensional axial speed of void boundary |
| $\Delta\zeta$ | axial mesh spacing |

**Acronyms**

| | |
|---|---|
| CBIC | cross-boundary interface continuity |
| CFM | computational fluid mechanics |
| ECA | Elrod's cavitation algorithm |
| JFO | Jakobsson-Floberg-Olsson |
| LGCMIED | liquid grid centered mesh integral emulation of divergence |
| OIC | Olsson's interphase condition |

## Author details

Coda H.T. Pan[1]* and Daejong Kim[2]

*Address all correspondence to: panwrites1@aol.com

1 Global Technology, Millbury, MA, USA

2 University of Texas at Arlington, Arlington, TX, USA

## References

[1] Floberg L. The infinite journal bearing, considering vaporization. In: Transactions of Chalmers University. Vol. 189. Göteborg, Sweden: Chalmers University of Technology; 1957

[2] Jakobsson B, Floberg L. The finite journal bearing, considering vaporization. In: Transactions of Chalmers University. Vol. 190. Göteborg, Sweden: Chalmers University of Technology; 1957

[3] Christopherson DG. A new mathematical method for the solution of film lubrication problems. Proceedings of the Institution of Mechanical Engineers, London. 1941;**146**:126

[4] Olsson KO. Cavitation in dynamically loaded bearings. In: Transactions of Chalmers University. Vol. 308. Göteborg, Sweden: Chalmers University of Technology; 1965

[5] Swift HW. The stability of lubricating films in journal bearings. Proceedings of the Institute of Civil Engineers. 1932;**233**:267-288

[6] Stieber W. Das Schwimmlager. Berlin: Verein Deutscher Ingenieure; 1933

[7] Braun MJ, Hannon WM. Cavitation formation and modelling for fluid film bearings: A review. Proceedings of the Institution of Mechanical Engineers, Part J. 2010;**224**:839-862

[8] Dowson D, Taylor CM. Fundamental aspects of cavitation in bearings. In: Proceedings of the 1st Leeds-Lyon Symposium on Tribology. Leeds, UK: University of Leeds; 1975. pp. 15-28

[9] Pan CHT, Kim TH, Rencis JJ. Rolling stream trails: an alternative cavitation analysis. ASME Journal of Tribology. 2008;**130**(2):021703

[10] Savage MD. Cavitation in lubrication. Part 1. On boundary conditions and cavity-fluid interfaces. Journal of Fluid Mechanics. 1977;**4**:743-755

[11] Sommerfeld A. Zur hydrodynamischen Theorie der Schmiermittehreibung. Zeitschrift für Angewandte Mathematik und Physik. 1904;**50**:97-155

[12] Gümbel L. Verleich der Ergebnisse der rechnerischen Behandlung des Lagerschmierungsproblem mit neueren Versuchsergebnissen. Mbl. Berl. Bez. (VDI). 1921:125-128

[13] Pan CHT. On Olsson's interphase condition in cavitation analysis. ASME Journal of Tribology. 2016;**137**(4):041704

[14] Michell AGM. Progress in fluid-film lubrication. Transactions of the ASME. 1929;**51**(2): 153-163

[15] Etsion I, Ludwig LP. Observation of pressure variation in the cavitation region of submerged journal bearings. ASME Journal of Tribology. 1982;**104**(2):157-163. DOI: 10.1115/1.3253174

[16] Press WH, Flannery BP, Teukolsky SA, Vetterling WT. Numerical Recipes: The Art of Scientific Computing. New York, NY: Cambridge University Press; 1986

[17] Kim D, Pan CHT. Spline-smoothing of **LGCMIED** computation in cavitation studies. ASME Journal of Tribology. 2019. Submitted for publication